Orientational ordering in sheared inelastic dumbbells

K. Anki Reddy,[1] V. Kumaran,[1] and J. Talbot[2]
[1]*Department of Chemical Engineering, Indian Institute of Science, Bangalore, 560012 India*
[2]*Laboratoire de Physique Théorique de la Matière Condensée, CNRS UMR 7600, Université Pierre et Marie Curie, 4 place Jussieu, 75252 Paris Cedex 05, France*
(Received 17 August 2009; published 24 September 2009)

Using even driven simulations, we show that homogeneously sheared inelastic dumbbells in two dimensions are randomly orientated in the limit of low density. As the packing fraction is increased, particles first tend to orient along the extensional axis, and then as the packing fraction is further increased, the alignment shifts closer to the flow axis. The orientational order parameter displays a continuous increase with packing fraction and does not appear to exhibit a universal scaling with elongation. Except at the highest packing fractions, the orientational distribution function can be reconstructed with only the first coefficient of the Fourier expansion.

DOI: 10.1103/PhysRevE.80.031304 PACS number(s): 45.70.Mg, 47.70.−n, 45.05.+x

I. INTRODUCTION

Molecular shape has a strong influence on the structural and dynamic properties of molecular fluids. There is always some degree of local orientational ordering and, for sufficiently elongated molecules, long-range orientationally ordered phases, such as the nematic phase, appear in the phase diagram. These phases may occur even in hard particle systems with no attractive interactions and can be explained by entropy maximization arguments. The effect of particle shape on the behavior of granular systems is, in contrast, largely unexplored. Granular systems are, of course, fundamentally different from their thermal (equilibrium) counterparts in many ways. They are composed of inelastic particles, in which energy is dissipated at each collision. In order to maintain the flow, a source of energy, such as a shear, must be present.

Recently, a density dependent nematic to smectic-like transition was observed for vibrated granular rods [1]. Also, a density-dependent isotropic-nematic transition, consistent with theory and simulation, has been found for vibrated rod-shaped granular materials confined to quasi-two-dimensional (2D) containers [2]. Narayan *et al.* [3] presented experimental evidence for giant number fluctuations in a monolayer of fluidized rods, although similar behavior has also been observed in systems of spherical particles [4]. All of these studies have been carried out in boundary-driven systems, where the energy supply is due to vibration at the boundaries. It is of interest to investigate other instances of granular systems composed of nonspherical particles, and sheared systems are of particular interest due to their relevance for numerous applications.

It has long been known that shear tends to align molecules. Indeed, Maxwell first studied the phenomenon over a century ago [5] by observing the optical bifringence that results from the alignment. Doi proposed a kinetic theory for the orientation of rod-like polymers in a homogeneous flow field [6], which was extended to investigate the effect of flow on the isotropic-nematic phase transition [7]. There are also hydrodynamic theories of nematic systems [8,9] and nonequilibrium molecular dynamics simulations of linear [10] and short chain molecules [11,12] and nematic fluids [13] under shear. As intuitively expected, shear tends to align the molecules along the extensional axis, and the orientational probability distribution shows a maximum along the extensional axis and a minimum along the compressional axis.

In these molecular systems, significant alignment is obtained only at very high-shear rates, or very close to phase boundaries. This can be rationalized as follows. The orientational effect of shear is due to the difference in the mean molecular velocities across a distance comparable to the molecular length scale in liquids. This tendency to orient is disrupted by the thermal fluctuating velocities of the molecules. The thermal velocities of (large) molecules are typically in the range of 100 m/s at room temperature. In contrast, even at very high-strain rates of $10-100\ s^{-1}$, the product of the particle diameter and the strain rate is at most of the order of 10^{-5} m/s (a slightly different argument using mean free paths should be applied to gases). Therefore, the alignment effect due to shear is likely to be small in practical applications, unless the system is already close to a nematic transition in liquids, or unless the flow speed is close to the speed of sound in gases.

Granular systems are crucially different from molecular systems, however, in that the shear rate and fluctuating velocity are no longer independent, but are related by an energy balance. The consequence is that shear rate can never be considered small unless the system is nearly elastic [14].

In contrast to the extensive body of work on sheared molecular systems, there are few studies of granular systems composed on anisotropic particles under shear, despite their acknowledged importance in industrial settings. In a recent article, Cleary [15] used the discrete element method (DEM) to explore the effect of particle shape on flow in a Couette shear cell. The particle geometry was described by a superquadric, $x^N+(y/A)^N=s^N$ where A is the aspect ratio of a particle with semimajor axis s and N characterizes the "blockiness" of the particle. The shear was induced by moving walls and a linear spring dashpot was used to model the normal and tangential forces during the particle-particle and particle-wall collisions.

Here, we study the effect of boundary driven shear on the orientational alignment of a two-dimensional system of inelastic dumbbells. In contrast to Cleary's study, we use hard particles that undergo instantaneous collisions. Also, instead

of physical walls we generate shear with the periodic boundaries, which leads to a homogeneous steady state.

The equilibrium phase behavior of two-dimensional hard rod fluids is quite subtle. Frenkel and Bates [16] concluded, however, that short rod systems do not exhibit a nematic phase, but undergo a transition directly from the solid to an isotropic phase. We expect this to be the case for the hard dumbbell system and indeed the results that we obtain are consistent with the lack of a nematic phase. This allows us to focus on the effect of shear on the orientational alignment in the absence of an underlying phase transition. We study how the dumbbells orient with respect to the flow field in a homogeneous shear flow, and we investigate the effect of elongation, packing fraction and inelasticity on the degree of alignment. A future article will discuss the dynamic properties of the system.

II. COLLISION MODEL AND SIMULATION METHODOLOGY

Granular flows of hard spherical particles (particles in which the pair potential is infinite when there is overlap, and zero otherwise), have been simulated by the event driven (ED) method. The ED method is used to simulate instantaneous collisions between hard particles, where the simulation proceeds in discrete collision events, instead of the fixed time intervals used in molecular dynamics for molecules with continuous potentials. In this procedure, the time required for the collision of two spherical particles i and j of diameter D with positions $\mathbf{r}_i$ and $\mathbf{r}_j$ and velocities $\mathbf{v}_i$, $\mathbf{v}_j$ can be obtained by solving the quadratic equation

$$\mathbf{v}_{ij}^2 t_{ij}^2 + 2(\mathbf{r}_{ij} \cdot \mathbf{v}_{ij}) t_{ij} + \mathbf{r}_{ij}^2 - D^2 = 0, \tag{1}$$

where $\mathbf{r}_{ij}=\mathbf{r}_i-\mathbf{r}_j$ is the separation vector at zero time, $\mathbf{v}_{ij}=\mathbf{v}_i-\mathbf{v}_j$ is the relative velocity, and D, the particle diameter, is the separation of the two particles at collision. Only the positive real roots t_{ij} of the above equation correspond to real future collisions, and the impending collision among all the particles is the one that occurs in the shortest time. The formulation of the ED algorithm is considerably simplified by the fact that Eq. (1) for the collision time is quadratic, which can be solved quite easily. In the case of nonspherical particles, however, it is necessary to solve a transcendental equation for the collision time of the form $f(t)=0$ rather than a polynomial equation. The procedure also has to be efficient and should accurately capture all the collisions that take place. A standard approach to solving algebraic equations involves combining the Newton-Raphson method with interval bisection. For the Newton-Raphson method, we also require the time derivative of the transcendental equation. To prevent the search for roots being totally open ended, it is convenient to enclose each particle in a circumscribing sphere and to seek collisions only while the spheres overlap. This means solving an equation like Eq. (1) so as to define the time interval of interest. We are still left with the problem of locating subintervals of time in which collisions can be shown either to occur (i.e., in which $f(t)$ changes sign) or not to occur.

We employ the method of retrospective collision detection first proposed by Rebertus and Sando [17] and developed by Allen *et al.* [18]. To summarize how this method works, the configuration is advanced on a regular step-by-step basis, just as in standard continuous-potential molecular dynamics, but using free-flight without collision. At the end of each step, the configuration is examined for overlapping pairs of molecules. For each overlapping pair, the collision equation is solved retrospectively to find the time at which collision should have occurred. The system is rewound to the point of collision, collision dynamics implemented, and the system is advanced to the end of the step. The configuration is then examined again to see if, after this, there is overlap. If such an overlap is detected the step is immediately abandoned, and the original configuration is restored. In this occurs the timestep is halved. If no overlap is detected, the routine goes on to consider the next colliding pair, and so on through the whole list. If all the collisions on the list are tackled successfully, the system will be moved to next time step. The complicated (although not very time consuming) part consists of handling multiple overlaps and resolving sequences of (possibly) inter-dependent collisions occurring within a very short time of each other. Full details on the simulation procedure can be found in Allen *et al.* [18].

The inelastic hard disk model has been used extensively for spherical particles with a constant coefficient of restitution. We extended the collision equations to inelastic nonspherical particles as follows. Consider two dumbbells with linear velocities $\mathbf{v}_1$ and $\mathbf{v}_2$ and angular velocities ω_1 and ω_2. Then, the total precollisional relative velocity at contact is,

$$\mathbf{g}_{12} = \mathbf{v}_{12} + \omega_1 \times \mathbf{r}_{c1} - \omega_2 \times \mathbf{r}_{c2}, \tag{2}$$

where $\mathbf{v}_{12}=\mathbf{v}_1-\mathbf{v}_2$. During collision, the components of $\mathbf{g}_{12}$ change such that,

$$(\mathbf{n} \cdot \mathbf{g}'_{12}) = -e_n(\mathbf{n} \cdot \mathbf{g}_{12})$$

$$(\mathbf{I} - \mathbf{nn}) \cdot \mathbf{g}'_{12} = (\mathbf{I} - \mathbf{nn}) \cdot \mathbf{g}_{12},$$

where $\mathbf{n}$ is the unit vector along the centerline of the two-sphere segments in the dumbbell that are colliding, and primed quantities denote values after collision. The parameter e_n is the normal coefficient of restitution. The linear and angular momentum change of the two particles in a collision can be written as,

$$\mathbf{p}'_1 = \mathbf{p}_1 + \Delta\mathbf{p}$$

$$\mathbf{p}'_2 = \mathbf{p}_2 - \Delta\mathbf{p}$$

$$\mathbf{J}'_1 = \mathbf{J}_1 + \mathbf{r}_{c1} \times \Delta\mathbf{p}$$

$$\mathbf{J}'_2 = \mathbf{J}_2 - \mathbf{r}_{c2} \times \Delta\mathbf{p}.$$

where

$$\Delta p = \frac{-(1+e_n)\mathbf{g}_{12} \cdot \mathbf{n}}{2/m + (\mathbf{r}_{c1} \times \mathbf{n})^2/I + (\mathbf{r}_{c2} \times \mathbf{n})^2/I},$$

where I is the moment of inertia and $\Delta\mathbf{p}=\mathbf{n}\Delta p$. The case $e_n=1$ corresponds to perfectly smooth elastic particles, where the component of the relative velocity along the line joining the centers of the particles is reversed in a collision.

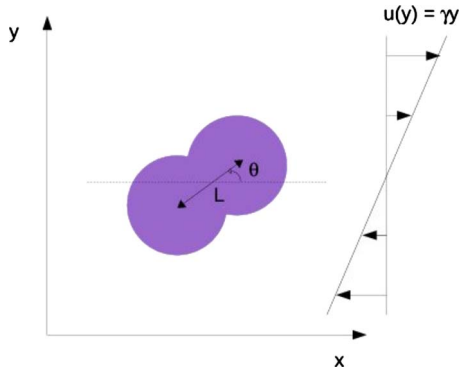

FIG. 1. (Color online) A dumbbell consists of two fused disks of diameter D with centers separated by a distance L. The Lees-Edwards boundary conditions induce a uniform shear in the sense shown. The orientation of the dumbbell with respect to the x axis is denoted by θ

The kinetic energy of the particles is unchanged in a collision for $e_n=1$, while there is a dissipation of energy for $e_n<1$.

We generate homogeneously sheared inelastic hard dumbbell configurations with a particular L/D ratio where L is the distance between the centers of the fused disks of a dumbbell and D is the diameter of the disk using the event-driven algorithm described above together with the Lees-Edwards boundary conditions [19]. The simulation box dimensions are l_x and l_y, both are of unit length. In our simulation geometry, x and y are the velocity gradient directions respectively: see Fig. 1. The top and the bottom boxes move with velocities $+U$ and $-U$, respectively, with respect to the central box. When a particle crosses the top/bottom boundary of the central box with a horizontal velocity v_x, its image enters through the bottom/top with a horizontal velocity $(v_x)_{image}=v_x \mp U$. This induces shear at the top/bottom boundaries of the central box, which then propagates by collisions into the central box. For most of the results reported here, the number of dumbbells used is 216; however, we have checked system size dependence by carrying out some simulations with four times the box size and 864 dumbbells, and we find no significant variation between the larger and smaller systems. Some snapshots of the 216 particle systems at different area fractions are shown in Fig. 2.

If a system of elastic particles is subjected to shear, the temperature will gradually increase. In order to achieve a steady state, it is necessary to apply a thermostatting method such as rescaling the velocities between collisions [20]. In a granular fluid a thermostat is not necessary as energy is dissipated by each collision ($e_n<1$). A steady state is established when the rate of energy supply through shear balances the rate of energy dissipation. Using dimensional arguments (e.g., [14]), one can show that this leads to

$$\dot{\gamma}^2 = C(1-e_n^2)T/D^2, \tag{3}$$

where T denotes the mean square of the velocity fluctuations (the particle mass can be set equal to 1 without loss of generality), and C is a (dimensionless) function of packing fraction and aspect ratio.

If the system is homogeneously sheared, we expect to observe a linear velocity profile, $v_x=\dot{\gamma}y$, where $\dot{\gamma}$ is the shear rate, in the central box. In addition the area fraction and the stress tensor are expected to be constant. These dynamical variables were extracted by dividing the channel into ten bins of equal width, and averaging over all the particles within one bin. With this procedure, we average over 500 realizations for the average value for each bin, and each bin contains about 20 particles on average. Therefore, the averages are calculated over approximately 10^4 particles for each data point across the channel. In the simulations, we find a constant area fraction and a linear mean velocity profile to a very good approximation, as shown in Fig. 3 for $L/D=1.0$, e_n

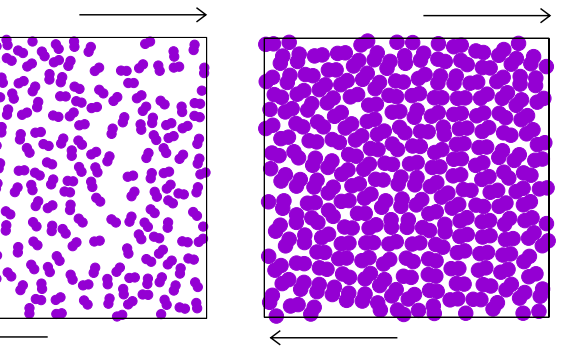

FIG. 2. (Color online) Sample configurations at packing fractions $\nu=0.4$ (left) and $\nu=0.8$ for coefficient of restitution $e_n=0.8$ and $L/D=1.0$.

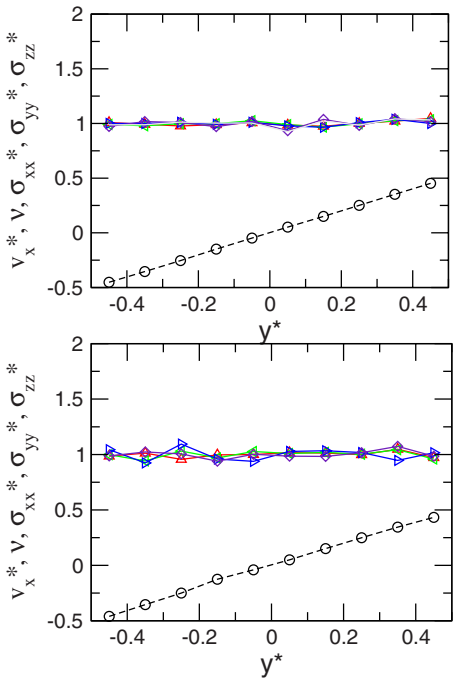

FIG. 3. (Color online) The average velocity $v_x^*=(v_x/\dot{\gamma}l_y)$ (○), the scaled area fraction $\nu^*=(\nu/\bar{\nu})$ (△), the scaled components of the stress $\sigma_{xx}^*=(\sigma_{xx}/\bar{\sigma}_{xx})$ (◁), $\sigma_{yy}^*=(\sigma_{yy}/\bar{\sigma}_{yy})$ (▷), $\sigma_{zz}^*=(\sigma_{zz}/\bar{\sigma}_{zz})$ (◇), as a function of distance across the channel $y^*=(y/l_y)$ for $L/D=1$, $e_n=0.8$ and for average area fraction $\nu=0.1$ (top) and $\nu=0.7$ (bottom). Here, l_y is the height of the simulation box which has been divided into ten equal bins, and the over bars represent averages over the entire box. The dashed line shows the expected linear velocity profile $v_x^*=(y/l_y)$.

=0.8 and for two different values of the area fraction. All the components of the stress tensor are constant across the channel.

III. RESULTS AND DISCUSSION

After an initial relaxation period, we observed a linear velocity profile with a shear rate $\dot{\gamma}=U/l=5.0$. Since there is no material time scale characterizing the collision, time can be scaled by the inverse of the strain rate. The only parameters affecting the flow dynamics are the length and diameter of the dumbbells, the packing fraction and the coefficient of restitution. Furthermore, there should be no modification in the system dynamics if all times are scaled by the inverse of the strain rate. We have checked this in the simulations by increasing the strain rate by a factor of 5, and verifying that the system dynamics is unaltered. Most of the results reported here are for $N=216$, although we also increased the system size by a factor of 4 and observed no significant changes. We performed approximately 1000 collisions per particle to allow the system to reach a steady state, followed by a further 2000 collisions per particle during which we computed properties. To verify that a homogeneous shear is present, we plotted velocity profiles as a function of height of the simulation box for all the parameter ranges described in this work. All were found to be linear. The stress tensor components, granular temperature and density are also uniform throughout the system. The variation of these quantities with inelasticity, area fraction and L/D ratio will be reported in a separate publication. Here, we focus on the order parameter and the orientational distribution. The geometry of a dumbbell and the coordinates used to specify its position and orientation are shown in Fig. 1. Sample snapshots are shown in Fig. 2.

We investigated the orientational order in the system by calculating the matrix

$$Q_{\alpha\beta}=\frac{1}{N}\left\langle \sum_{i=1}^{N}(2u_{\alpha i}u_{\beta i}-\delta_{\alpha\beta})\right\rangle, \tag{4}$$

where $u_{\alpha i}$ denotes the component α of the unit vector specifying the direction of the i^{th} dumbbell and the angular brackets denote an average over a (large) number of configurations at equally spaced time intervals. The matrix Q has two eigenvalues, $\pm S$, the largest of which corresponds to the order parameter. In a perfectly orientationally ordered system $S=1$, while in the isotropic phase (for an infinite system) $S=0$. First we examine the order parameter as a function of area fraction for different L/D ratios. The order parameter as a function of inelasticity and elongation is shown in Figs. 4 and 5, respectively.

We see from Figs. 4 and 5 that there is a continuous increase in the ordering as the elongation is increased, or the coefficient of restitution is decreased. Figure 6 shows the order parameter as a function of packing fraction for three different system sizes ($N=216$, 432, and 864). The ordering increases with increasing packing fraction and it is also apparent that there is little, if any, effect of system size.

The increase in ordering with packing fraction is easy to understand on the basis of packing constraints. The increase

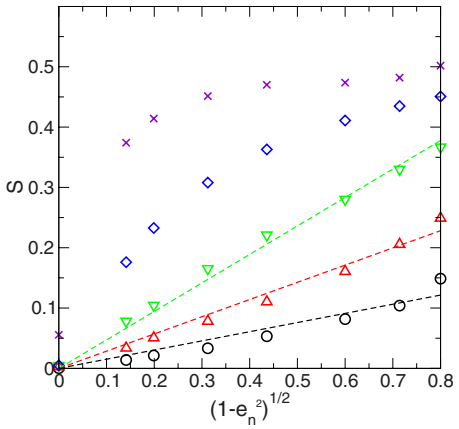

FIG. 4. (Color online) The order parameter S as a function of $(1-e_n^2)$ for $L/D=1.0$ and for packing fractions $\nu=0.3$ (○), $\nu=0.4$ (△), $\nu=0.5$ (▽), $\nu=0.6$ (◇), $\nu=0.7$(×), The curves show best fits of the form $S=B(1-e_n^2)^{1/2}$.

in ordering with inelasticity can be understood as follows. For a steady shear flow, there is a balance between the rate of production of fluctuating energy due to mean shear and the rate of dissipation due to inelastic collisions. From the energy balance condition, Eq. (3), we see that if we decrease the coefficient of restitution at constant packing fraction and aspect ratio, the fluctuating velocity decreases at constant shear rate. Since velocity fluctuations tend to randomize the system whereas the mean shear tends to align particles in the flow direction, a decrease in the coefficient of restitution increases ordering in the system.

We can deduce from Eq. (3) that the limit $e_n\to 1$ corresponds to an elastic system with no shear. An interesting feature of Fig. 4 is that the order parameter decreases to zero in this limit. Therefore, we conclude that for all the L/D ratios and packing fractions studied here, there is no spontaneous symmetry breaking and order/disorder transition in the absence of shear, an observation that is consistent with a theoretical analysis of the planar dumbbell fluid [21] and also with simulation studies of the 2D spherocylinder fluid [16], a

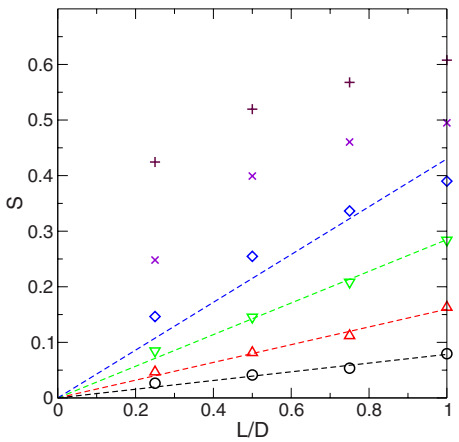

FIG. 5. (Color online) The order parameter S as a function of L/D for $e_n=0.80$ and for packing fractions $\nu=0.3$ (○), $\nu=0.4$ (△), $\nu=0.5$ (▽), $\nu=0.6$ (◇), $\nu=0.7$(×). $\nu=0.8$(+). The curves show best fits of the form $S=A(L/D)$.

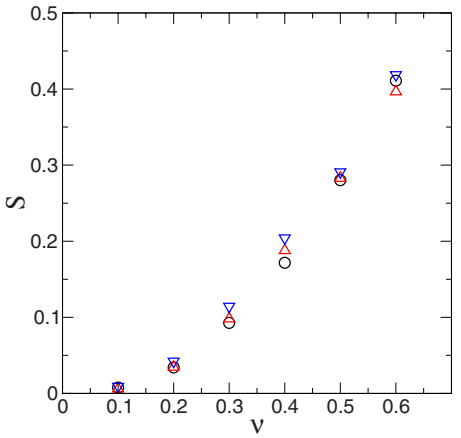

FIG. 6. (Color online) The order parameter S as a function of packing fraction ν for different system sizes: $N=216$ (○), $N=432$ (△), $N=864$ (▽). $L/D=1$ and $e_n=0.8$.

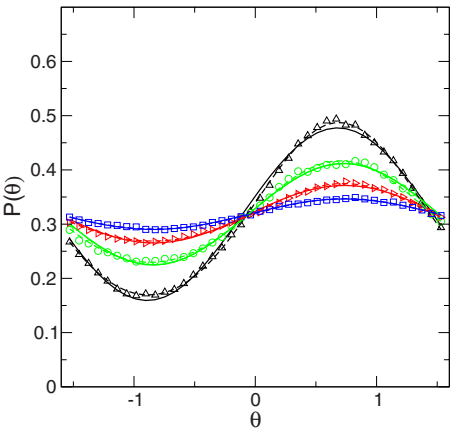

FIG. 7. (Color online) The orientational distribution function, $P(\theta)$, at $L/D=0.25$, $e_n=0.8$, for packing fractions 0.7, 0.6, 0.5, and 0.4 in order of decreasing amplitude. The solid and dashed lines show the reconstruction of the function using the first term, a_1, and the first two terms, a_1 and a_2, of the Fourier expansion, respectively.

closely related system for $L/D \leq 1$. The increase in ordering that we observe is due solely to the imposition of a shear flow.

Based on the competition between the shear, which tends to align particles, and the fluctuating velocity, which randomizes orientation, we would expect S to be a function of the variable $\dot{\gamma}D/T^{1/2}$. From the energy balance, Eq. (3), we expect that $S \propto (1-e_n^2)^{1/2}$. For packing fractions of less than about 0.5 this expression does provide a good representation of the simulation data for S: See Fig. 4. At higher packing fractions, significant deviations from linearity are observed.

The curves in Fig. 5 are fits of $S=A(L/D)$, which is the expected behavior for small L/D if S has an analytic dependence on L/D. This linear fit describes the behavior for packing fraction up to about 0.5. However, at higher packing fractions beyond about 0.5, curvature is evident.

While the order parameter S gives an averaged estimate of the alignment, more detailed information is provided by the orientational probability distribution function, $P(\theta)$ (where $\theta=\tan^{-1}(u_y/u_x)$ is the angle shown in Fig. 1) and $P(\theta)d\theta$ is the probability that the angle lies between θ and $\theta+d\theta$. The orientational distribution functions for $e_n=0.8$ are shown in Fig. 7 (for $L/D=0.25$) and Fig. 8 (for $L/D=1.0$). At low-packing fraction, the distribution is nearly uniform, implying that there is no preferred orientation. As the packing fraction increases the distribution becomes more peaked with a maximum at θ_p and a minimum at $\theta_p-\pi/2$. These distributions are qualitatively similar to those obtained by Rapaport [11] in simulations of short chain molecules in pipe flow. At low-packing fraction, the maximum and minimum are close to the extension axis ($\theta_p=\pi/4$) and compression axes, respectively. As the packing fraction increases, the preferred orientation shifts progressively to smaller angles (closer to the flow direction), with the minimum following. This behavior can be confirmed by computing $\tan\theta_p=e_y/e_x$ where e_x and e_y are the components of the normalized eigenvector (See Fig. 9).

Since $P(\theta)$ evolves in a self-similar manner, we attempt to express it in the form of a Fourier expansion,

$$P(\theta) = \frac{1}{\pi} + \sum_{n=1}^{\infty} a_n \cos[2n(\theta-\theta_p)], \tag{5}$$

where the first term $(1/\pi)$ on the right side is due to the normalization condition $\int_{-\pi/2}^{\pi/2} P(\theta)d\theta=1$. The other Fourier coefficients can be calculated using the orthogonality relations

$$a_n = \frac{2}{\pi}\int_{-\pi/2}^{\pi/2} P(\theta)\cos[2n(\theta-\theta_p)]d\theta. \tag{6}$$

It can easily be verified that the first coefficient a_1 is related to the orientational order parameter by $a_1=(2S/\pi)$. The connection is established starting from $u_x=\cos\theta$, $u_y=\sin\theta$ and the definition of Q, Eq. 3.1.

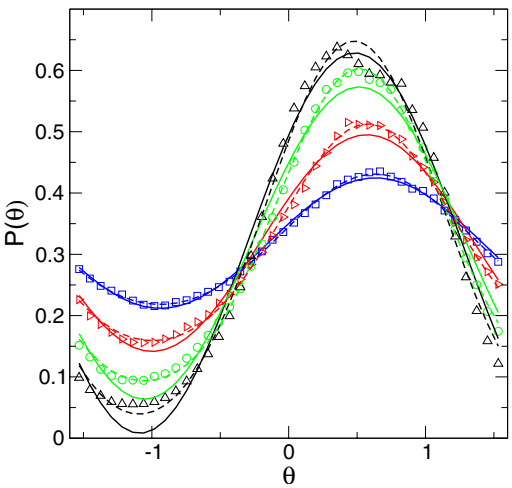

FIG. 8. (Color online) Same as Fig. 6, except $L/D=1.0$

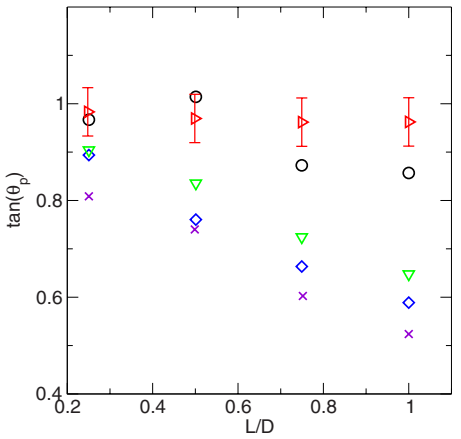

FIG. 9. (Color online) $\tan(\theta_p)$ as a function of L/D for $e_n=0.8$ at different packing fractions: $\nu=0.2$(▷), $\nu=0.3$ (○), $\nu=0.5$ (▽), $\nu=0.6$ (◇), $\nu=0.7$(×). Error estimates are shown for $\nu=0.2$. The errors are smaller at higher packing fractions.

$$Q_{xx} = \langle 2u_x^2 - 1 \rangle = \int_{-\pi/2}^{\pi/2} (2\cos^2\theta - 1)P(\theta)d\theta = \frac{\pi}{2}a_1 \cos 2\theta_p. \tag{7}$$

Similarly

$$Q_{yy} = \langle 2u_y^2 - 1 \rangle = \int_{-\pi/2}^{\pi/2} (2\sin^2\theta - 1)P(\theta)d\theta = -\frac{\pi}{2}a_1 \cos 2\theta_p \tag{8}$$

and

$$Q_{xy} = Q_{yx} = \langle 2u_y u_x \rangle = \frac{\pi}{2}a_1 \sin 2\theta_p. \tag{9}$$

The eigenvalues of the matrix Q are

$$\lambda = \pm\sqrt{Q_{xx}^2 + Q_{xy}^2} = \pm\frac{\pi}{2}a_1 \tag{10}$$

so that $S=(\pi/2)a_1$. The corresponding eigenvectors are

$$\begin{pmatrix} \cos\theta_p \\ \sin\theta_p \end{pmatrix} \text{ and } \begin{pmatrix} -\sin\theta_p \\ \cos\theta_p \end{pmatrix}. \tag{11}$$

We have obtained the values of a_1, a_2, and θ_p by a nonlinear fit of the Fourier expansion, Eq. (5), truncated to second order to the numerical simulation data. Some numerical values are presented in Table I. We observe that the coefficients a_1 and a_2 increase with packing fraction at constant L/D and with L/D at constant packing fraction. For the simulations reported here, the ratio (a_2/a_1) has a maximum of about 0.1 at the highest area fractions and the lowest coefficients of restitution examined here. This indicates that the orientational distribution function is well described by just the first term in the Fourier expansion, i.e., a simple cosine function; all higher terms in the expansion are numerically small.

TABLE I. Coefficients of the Fourier expansion of the orientational distribution function at various packing fractions. $e_n=0.8$

L/D	ν	$\tan(\theta_p)$	a_1	a_2
0.25	0.4	0.913	0.028	0.001
0.25	0.5	0.888	0.053	0.003
0.25	0.6	0.847	0.094	0.005
0.25	0.7	0.824	0.159	0.010
1.0	0.4	0.734	0.106	0.006
1.0	0.5	0.651	0.177	0.018
1.0	0.6	0.570	0.255	0.030
1.0	0.7	0.517	0.305	0.026

IV. DISCUSSION

Our simulations show that there is a continuous increase in the alignment of sheared inelastic dumbbells with increasing inelasticity, aspect ratio and packing fraction, but no discontinuity. Although there is no isotropic-nematic transition in the equilibrium 2D dumbbell systems with $L/D<1$, more elongated particles such as ellipses and spherocylinders do display such a transition. In *three dimensions* (3D), numerical simulation studies, most notably by Frenkel [22], indicated that there is a discontinuous isotropic-nematic transition for spheroids and spherocylinders with finite aspect ratios greater than about 2.5, as well as a nematic-smectic transition in spherocylinders. At present, it is still not clear whether the imposition of shear would have a qualitative effect on these transitions, and whether the ordered state would be dynamically stable. While one might intuitively expect that shear will have only a quantitative effect on the transition, studies on hard sphere systems indicate ordering is completely destroyed by the presence of shear. In a system of hard spheres in three dimensions, there is a crystallization transition at a packing fraction of 49% in the absence of shear. However, in the presence of shear, it is found that there is no ordering transition, and the system continues to be in the random state even as the random close packing-packing fraction is approached [23]. It is possible that shear may have a similar effect on the isotropic-nematic transition in 3D hard anisotropic particle systems.

ACKNOWLEDGMENTS

We thank P. Viot for useful discussions. This research was supported by the Department of Science and Technology, Government of India.

[1] D. L. Blair, T. Neicu, and A. Kudrolli, Phys. Rev. E **67**, 031303 (2003).
[2] J. Galanis, D. Harries, D. L. Sackett, W. Losert, and R. Nossal, Phys. Rev. Lett. **96**, 028002 (2006).
[3] V. Narayan, S. Ramaswamy, and N. Menon, Science **317**, 105 (2007).
[4] I. S. Aranson, A. Snezhko, J. S. Olafsen, and J. S. Urbach, Science **320**, 612c (2008).
[5] J. C. Maxwell, Proc. R. Soc. London **22**, 46 (1873).
[6] M. Doi, J. Polym. Sci. Polym. Phys. Ed. **19**, 229 (1981).
[7] H. See, M. Doi, and R. Larson, J. Chem. Phys. **92**, 792 (1990).
[8] P. D. Olmsted and P. Goldbart, Phys. Rev. A **41**, 4578 (1990).
[9] R. G. Larson, Macromolecules **23**, 3983 (1990).
[10] T. Weider, U. Stottut, W. Loose, and S. Hess, Physica A **174**, 1 (1991).
[11] D. C. Rapaport, Europhys. Lett. **26**, 401 (1994).
[12] Y. Radzyner and D. C. Rapaport, Phys. Rev. E **57**, 5687 (1998).
[13] S. Sarman and D. J. Evans, J. Chem. Phys. **99**, 9021 (1993).
[14] I. Goldhirsch, Annu. Rev. Fluid Mech. **35**, 267 (2003).
[15] P. W. Cleary, Powder Technol. **179**, 144 (2008).
[16] M. A. Bates and D. Frenkel, J. Chem. Phys. **112**, 10034 (2000).
[17] W. Rebertus and K. M. Sando, J. Chem. Phys. **67**, 2585 (1977).
[18] M. P. Allen, D. Frenkel, and J. Talbot, Comput. Phys. Rep. **9**, 301 (1989).
[19] A. W. Lees and S. F. Edwards, J. Phys. C **5**, 1921 (1972).
[20] D. J. Evans and B. L. Holian, J. Chem. Phys. **83**, 4069 (1985).
[21] Sz. Varga and I. Szalai, J. Mol. Liq. **85**, 11 (2000).
[22] D. Frenkel, J. Phys. Chem. **91**, 4912 (1987).
[23] V. Kumaran, J. Fluid Mech. **632**, 109 (2009); **632**, 145 (2009).